Neuron, Vol. 29, 657–667, March, 2001, Copyright ©2001 by Cell Press

Yeast Screen for Constitutively Active Mutant G Protein–Activated Potassium Channels

B. Alexander Yi, Yu-Fung Lin, Yuh Nung Jan, and Lily Yeh Jan*
Departments of Physiology and Biochemistry
Howard Hughes Medical Institute
University of California, San Francisco
533 Parnassus Avenue
San Francisco, California 94143

Summary

GIRK2 is a major contributor to G protein–activated inward rectifier potassium channels in the mammalian brain. How GIRK channels open upon contact with Gβγ remains unknown. Using a yeast genetic screen to select constitutively active mutants from a randomly mutagenized GIRK2 library, we identified five gating mutations at four residues in the transmembrane domain. Further mutagenesis indicates that GIRK channel opening involves a rotation of the transmembrane segments, bringing one of these residues (V188) to a pore-lining position in the open conformation. Combined with double-mutant studies, these findings suggest that GIRK channels gate by moving from the open conformation inferred from our yeast study of Kir2.1 to a closed conformation perhaps resembling the known KcsA structure.

Introduction

The term "gating" refers to the conformational changes associated with the opening and closing of ion channels. This implies that ion channels can adopt (at least) two structural forms representing an open state and a closed state. Owing to the dynamic nature of gating, the mechanism by which ion channels open and close remains elusive and an area of great interest.

G protein–activated potassium channels (GIRK/Kir3.0), a well-characterized class of ion channels, belong to the family of inwardly rectifying K^+ channels that are gated by their interaction with G proteins (Jan and Jan, 1997). In vivo, the activation of G protein–coupled receptors releases Gβγ that binds directly to cytoplasmic regions of GIRK channels (Wickman et al., 1994; Huang et al., 1997) causing the open probability of a GIRK channel to increase from less than 0.01 to 0.05–0.1 (Ivanova-Nikolova and Breitwieser, 1997; Nemec et al., 1999; Yakubovich et al., 2000). This pathway of channel activation is known to underlie the generation of inhibitory postsynaptic potentials in the brain (Lüscher et al., 1997; Guatteo et al., 2000) and the slowing of the heart rate following parasympathetic stimulation (Wickman et al., 1998). Little is known, however, about the last steps in this process—for example, how does the binding of Gβγ induce GIRK channels to open? An immediate and relevant question is "what are the structural rearrangements that GIRK channels undergo during gating?"

Inwardly rectifying K^+ channels share the same basic M1-P-M2 membrane topology with the bacterial K^+ channel KcsA, i.e., two transmembrane segments separated by a P loop with the N and C terminus residing in the cytoplasm (Doyle et al., 1998). In this architecture, M2 forms the inner helix, which lines the pore, while M1 is arrayed around the inner helices and faces the membrane bilayer. The P loop contains the pore helix and the GYG motif and determines the selectivity of the ion channel for K^+. It takes four subunits to form a functional channel. Beyond general similarities, however, it is unclear how well the KcsA structure will correspond to the structure of inwardly rectifying K^+ channels. Sequence analysis and sensitivity to K^+ channel toxins suggest that KcsA resembles more closely the pore of voltage-gated K^+ channels than inward rectifiers (MacKinnon et al., 1998). Furthermore, mutational analysis of yeast selection studies has been used to propose an arrangement of M1 and M2 in IRK1 (Kir2.1) distinct from that of KcsA (Minor et al., 1999). Nevertheless, KcsA remains an important and useful model from which to derive insights of inward rectifiers (Capener et al., 2000; Thompson et al., 2000) as well as members of other distantly related ion channels.

There is little known about the location of the gate or the structural changes associated with GIRK channel gating. One model is that the C terminus acts as a blocking particle that makes reversible interactions with the pore (Pessia et al., 1995; Luchian et al., 1997). However, since the C terminus contains the putative binding site for Gβγ, PIP_2, and Na^+ as well as sequence motifs that regulate membrane trafficking (Huang et al., 1998; He et al., 1999; Ho and Murrell-Lagnado, 1999; Kennedy et al., 1999), it is conceivable that this region could have other effects that influence channel activity. In Kir6.2, studies of mutations identified by site-directed mutagenesis in the second half of M2 suggest that the gate is located near the intracellular end of the pore (Drain et al., 1998; Tucker et al., 1998), in step with models of voltage-gated K^+ channel gating (Liu et al., 1997) and the pH-dependent gating of KcsA (Perozo et al., 1999).

We undertook a yeast genetic screen from a randomly mutated GIRK2 library as an unbiased method of rapidly screening hundreds of thousands of mutations for those that affect the gating of GIRK2. In *S. cerevisiae*, high-affinity K^+ uptake is dependent on the K^+ transporters TRK1 and TRK2 (Ko and Gaber, 1991). Strains of yeast that lack TRK1 and TRK2 grow only on media supplemented with high concentrations of K^+. Growth on low K^+ media can be restored by the heterologous expression of certain inwardly rectifying K^+ channels that allow K^+ to directly enter the cell. One such channel is the constitutively active inward rectifier IRK1 (Tang et al., 1995; Minor et al., 1999).

Having subjected the entire GIRK2 sequence to random mutagenesis, we found mutations of four residues in the transmembrane domain that exhibit dramatic ef-

*To whom correspondence should be addressed (e-mail: gkw@itsa.ucsf.edu).

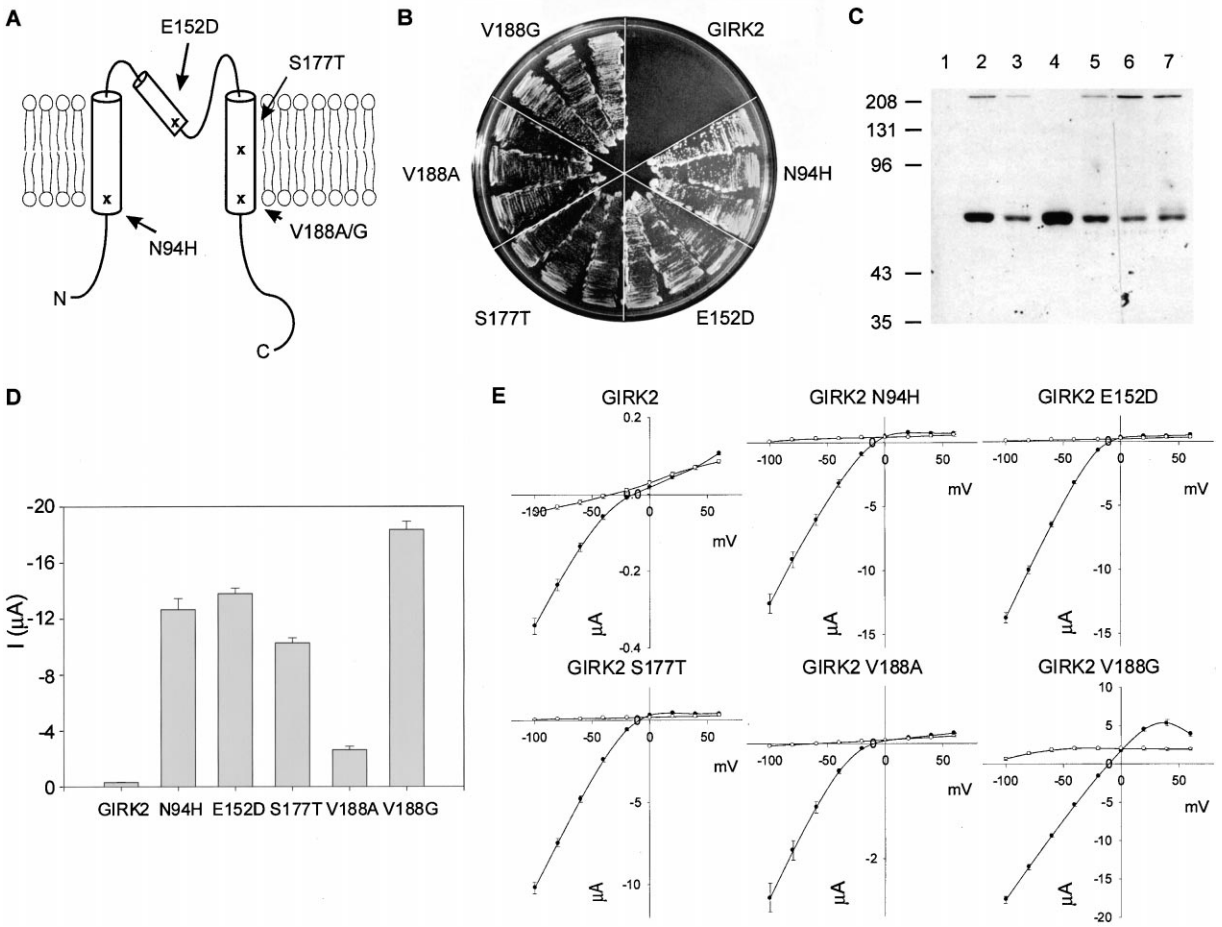

Figure 1. Mutations in GIRK2 Identified by Selection among a Randomly Mutagenized GIRK2 Library for Those that Rescue Yeast Growth

(A) A schematic representation of a GIRK2 subunit showing the locations of mutations.

(B) Growth phenotype of yeast expressing GIRK2 or single mutants on a plate supplemented with 0.1 mM KCl.

(C) Protein expression levels of mutants in *Xenopus* oocytes. The predicted mass of GIRK2 monomer is 47.5 kDa. Protein isolated from oocytes were loaded as follows: 1, uninjected oocytes; 2, GIRK2; 3, N94H; 4, E152D; 5, S177T; 6, V188A; 7, V188G.

(D) Mean currents of mutant GIRK2 channels relative to wild-type GIRK2 in *Xenopus* oocytes measured at −100 mV in 90K bath solution (n = 5, error bars indicate SEM).

(E) Current-voltage plots of the GIRK2 mutants in high K^+ and high Na^+ bath solution. Two-electrode voltage-clamp currents were recorded from oocytes expressing GIRK2 or mutant channels and plotted as I-V plots. Closed circles show currents recorded in 90K bath solution and open circles show currents in 90Na bath. Points in the I-V curves represent mean ± SEM from oocytes isolated from the same batch.

fects on the gating of GIRK2 without disrupting its other properties. To investigate these residues further, we replaced each of these four residues one at a time with all other nineteen amino acids. One residue, V188, tolerates only substitution by hydrophobic residues of comparable size in the closed channel but can be replaced with any of the other residues in a constitutively open channel, suggesting that it faces the pore in the open channel but has to fit snugly within a hydrophobic pocket in the closed channel. It thus appears that the transmembrane domain undergoes substantial rotation as the channel opens and closes. Based on mutagenesis and single-channel analysis, one possible model for the gating movement is that GIRK channels gate by moving from an open conformation similar to Kir2.1 (Minor et al., 1999) to a closed state that may resemble the known structure for KcsA (Doyle et al., 1998).

Results

A Yeast Genetic Screen for Gating Mutations in GIRK2

In *Xenopus* oocytes, homomultimers of GIRK2 display small basal currents, while IRK1, a constitutively active inward rectifier, displays large currents. This difference in current expression can, in part, be attributed to the lower probability of opening (P_o) of GIRK2, which is <0.01, compared to that of IRK1, which is near one (Kubo et al., 1993). First, we determined whether complementation of the potassium uptake–deficient phenotype of a strain of *S. cerevisiae* could serve as an assay for the difference in current expression between GIRK2 and IRK1. After streaking on plates containing nominally low levels of K^+ (0.5 mM KCl), yeast transformed with IRK1 grew (Tang et al., 1995; Minor et al., 1999) while

Table 1. Summary of Single-Channel Properties

Properties	GIRK2	N94H	E152D	S177T	V188A	V188G
NP_o (%)	0.60 ± 0.17[a]	4.40 ± 1.03**	1.63 ± 0.39*	1.03 ± 0.29	4.42 ± 2.18*	6.44 ± 1.97**
Opening frequency (s^{-1})	10.88 ± 3.06	20.11 ± 5.77	15.00 ± 3.55	7.53 ± 1.90	33.10 ± 12.96*	28.30 ± 8.65*
Mean open duration (ms)	0.42 ± 0.04	2.31 ± 0.11***	1.05 ± 0.03***	1.34 ± 0.07***	1.32 ± 0.16***	2.22 ± 0.21***
Mean closed duration (ms)	197.80 ± 52.91	176.60 ± 64.15	132.50 ± 45.29	198.20 ± 44.22	83.52 ± 38.89	55.79 ± 16.65*
No. of openings	28,850	31,560	16,050	8,678	11,830	30,177
No. of patches	10	12	10	10	5	7

Recordings were made from cell-attached patches from *Xenopus* oocytes injected with cRNAs diluted to give single channels. Comparisons were made by performing one-way analysis of variance (ANOVA) on data obtained from GIRK2, GIRK2 N94H, GIRK2 E152D, GIRK2 S177T, GIRK2 V188A, and GIRK2 V188G channels and followed by Bonferroni's multiple comparison tests. Data are presented as mean ± SEM. Triple asterisk, $p < 0.0001$; double asterisk, $p < 0.005$; single asterisk, $p < 0.05$: other values were not statistically different from wild type.
[a] Because the number of channels for GIRK2 could be more than one due to the low open probability, the NP_o for GIRK2 is likely an overestimate.

yeast transformed with GIRK2 did not (Figure 1B). Expression of GIRK2 was confirmed by Western blotting (data not shown).

A library of randomly mutagenized GIRK2 was created using the method of DNA shuffling (Stemmer, 1994). DNA shuffling is a method of introducing mutations by random fragmentation of genes and reassembly using the polymerase chain reaction. Of ~200,000 transformants, 0.5% grew after being replica plated onto plates containing 0.1 mM KCl. Sequencing showed that, on average, each positive clone that rescued yeast growth had 9–10 mutations scattered throughout the GIRK2 coding sequence. To reduce the number of spurious mutations, ~100 positive clones were pooled and backcrossed with a 5-fold excess of wild-type GIRK2 sequence using a DNA shuffling protocol modified for higher fidelity (see Experimental Procedures). This reduced the number of mutations per positive clone to between three and four. Single mutations were further isolated until five mutations—N94H, E152D, S177T, V188A, and V188G—were identified that were individually sufficient to confer growth on 0.1 mM KCl plates (Figure 1B). Seven independent clones carried the V188A mutation, and six independent clones carried the V188G; the other mutations were found in one independent clone each. These mutations are located within the presumed transmembrane domain of GIRK2. N94 is located in M1, E152 in the P loop, and S177 and V188 in M2 (Figures 1A and 5A). Based on their predicted locations relative to the cytoplasmic surface of the membrane, N94 and V188 form an inner pair whereas E152 and S177 form an outer pair.

GIRK2 cRNA carrying these mutations were injected into *Xenopus* oocytes, and current amplitudes in 90K bath solution were measured and compared to wild type. GIRK2 mutant channels expressed 4- to 30-fold higher basal currents than wild type (Figure 1D), while leaving properties such as inward rectification and potassium selectivity unaltered (Figure 1E). No inward currents were observed in 90Na/0K bath solution. Western analysis of GIRK2 isolated from oocytes revealed two bands that correspond in size to the monomer and the undissociated tetramer (Figure 1C). The mutants carrying N94H, S177T, V188A, or V188G appeared to be expressed at slightly lower levels than wild type. GIRK2 E152D appeared to be expressed at levels higher than wild type, but this difference does not appear sufficient to fully account for the ~20-fold enhancement in current amplitudes observed. Overall, the mutations did not greatly affect levels of GIRK2 protein expression in oocytes.

Single-channel recordings were obtained to address whether these mutations affect the channel-gating properties of GIRK2. The mutations identified did not affect the single-channel conductance but profoundly changed the single-channel kinetic properties of GIRK2 (Table 1; Figure 2A). In oocytes, GIRK2 predominantly shows brief, flickery openings. For the mutant channels, the most striking change was the clustering of channel openings into long bursts separated by inactive periods with few openings. This prolonged bursting phenotype was most prominent in mutations of the inner pair, N94H or V188G, located near the cytoplasmic surface of the membrane. Mutations of the outer pair, E152D or S177T, also gave rise to bursts, though they were shorter than those seen with the inner pair. In addition, mutations of the outer pair exhibited subconductance openings that were not seen in other mutants, wild-type GIRK2, or uninjected oocytes (Table 1; Figure 2A). Like V188G, GIRK2 V188A channels displayed a higher frequency of opening, though the alanine substitution generated a weaker phenotype than the glycine substitution. All mutants exhibited increases in the NP_o and mean open duration of single-channel openings (Table 1), indicating that the mutations identified in the screen enhance GIRK2 currents by altering the gating properties of GIRK2. It is important to note that, owing to the low open probability of wild-type GIRK channels, it is difficult to ensure the presence of a single channel in the membrane patch. While the open probability is known to increase from less than 0.01 to 0.05–0.1 upon maximal stimulation (Ivanova-Nikolova and Breitwieser, 1997; Yakubovich et al., 2000), it is reduced by over 1000-fold by excess $G\alpha$-GDP (Nemec et al., 1999). Thus, the NP_o (0.006) for the wild-type channel is likely an overestimate due to the presence of multiple channels.

Kinetic analysis of GIRK activation suggests that GIRK channels fluctuate between modes of low and high activity (Ivanova-Nikolova et al., 1998; Yakubovich et al., 2000). The binding of $G\beta\gamma$ is thought to increase GIRK currents by favoring entry of channels into high-activity modes characterized by a high frequency of openings clustered into bursts (Figure 2B). The gating properties of wild-type GIRK channels activated by Na^+ or $G\beta\gamma$ (Ivanova-Nikolova and Breitwieser, 1997; Ivanova-Nikolova et al., 1998; Sui et al., 1998; Nemec et al., 1999) are

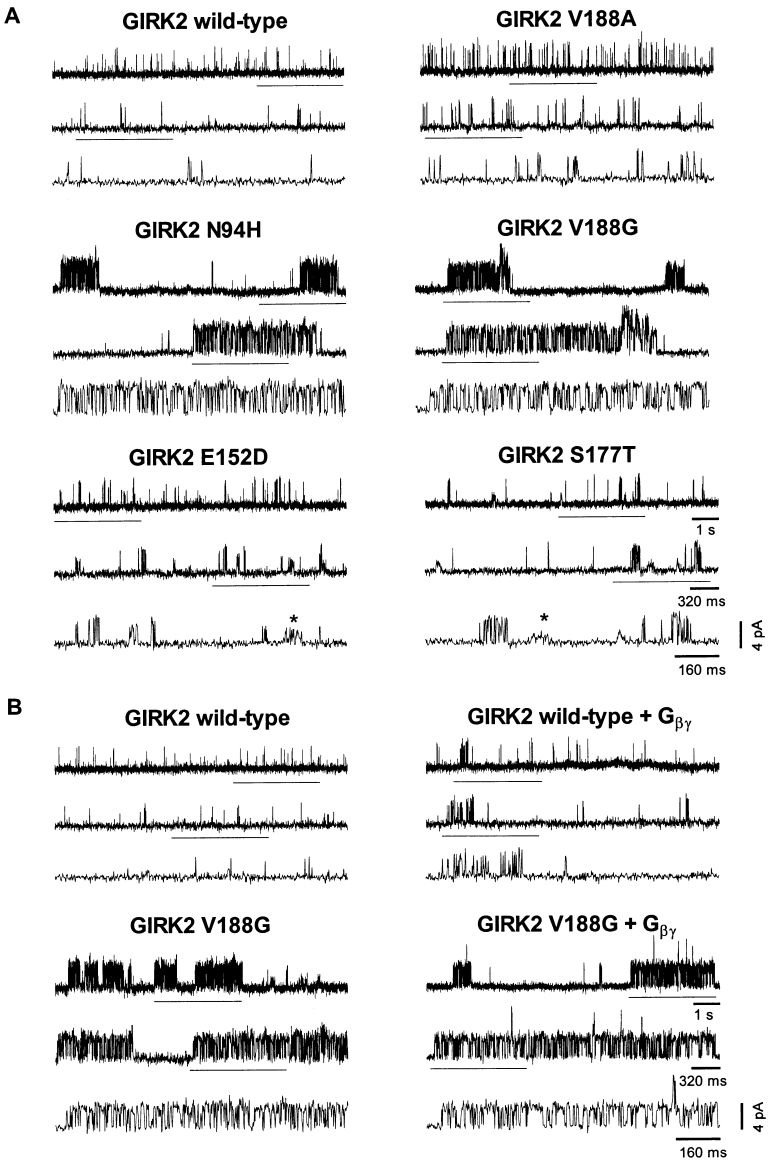

Figure 2. The Mutations Identified in the Yeast Screen Increase Channel Activity by Altering the Gating Properties of GIRK2

(A) Representative single-channel recordings of GIRK2 and the GIRK2 mutants were obtained in the cell-attached configuration from *Xenopus* oocytes at a holding potential of −100 mV. Examples of the subconductance states in GIRK2 E152D and GIRK S177T are marked with asterisks. Channel openings are upward deflections. Bars indicate traces shown in expanded time scales below.

(B) Single-channel records of GIRK2 and GIRK2 V188G expressed alone (left panels) or coexpressed with 2.5 ng of $G\beta_1$ and 2.5 ng of $G\gamma_2$ (right panels).

qualitatively similar to the mutant gating phenotypes observed here. Further analysis is necessary to establish a relationship between mutations at these positions and the modal gating behavior of GIRK channels. Unlike GIRK2 wild-type channels, V188G mutant channel activity was not reduced by coexpression of $G\alpha_i$ nor greatly enhanced by coexpression with $G\beta_1\gamma_2$ (Figure 2B and data not shown). These findings indicate that the mutation caused the channel to be constitutively active rather than becoming hypersensitive to $G\beta\gamma$ stimulation.

Profile of Amino Acid Substitutions

Substitution of V188 with the smaller alanine or glycine increased the open probability of GIRK2 leading to rescue of yeast growth and increased basal currents in *Xenopus* oocytes. Given the length of the GIRK2 sequence and the error rate obtained with DNA shuffling, it is unlikely that all amino acids at a particular position were represented in our library since some changes require two or three simultaneous base changes within a codon. We, therefore, replaced V188 with the other amino acids in order to determine the types of amino acid changes that were associated with high-current expression and, by extension, the open state of the channel.

All mutations were tested in the yeast assay and expressed in *Xenopus* oocytes. At V188, surprisingly, the majority of amino acid substitutions resulted in active channels (Table 2); 13 out of 20 amino acids both complemented the yeast phenotype and expressed large basal currents. Three additional mutations produced light growth on 0.1 mM KCl plates. L, F, I, and V (wild type)—amino acids that are hydrophobic—did not lead to yeast rescue. Thus, the mutant channel was highly active in both yeast and *Xenopus* oocytes if V188 was replaced with amino acids that are small (S, G, and A), polar (N, Q, S, T, and C), acidic (D and E), and basic (K, R, and H).

Table 2. Amino Acid Substitutions in GIRK2 Positions that Affect Gating

Mutation	Low K Growth	I (μA) Mean ± SEM	Sodium Current?	Mutation	Low K Growth	I (μA) Mean ± SEM	Sodium Current?
N94**H**	+	−8.95 ± 0.52	No	E152**D**	+	−16.37 ± 0.29	No
N94**F**	+	−3.05 ± 0.38	No	E152T	−	−11.99 ± 0.56	Yes
Wt	−	−1.04 ± 0.19	No	E152V	−	−8.05 ± 0.31	Yes
N94E	−	−0.54 ± 0.06	No	E152**Q**	+	−7.95 ± 1.0	No
N94Y	−	−0.36 ± 0.04	No	E152A	−	−7.66 ± 0.48	Yes
N94L	−	−0.32 ± 0.04	No	E152H	−	−7.34 ± 1.1	Yes
N94S	−	−0.25 ± 0.02	No	E152G	−	−4.60 ± 0.24	Yes
N94W	−	−0.25 ± 0.03	No	E152S	−	−2.24 ± 0.53	No
N94D	−	−0.13 ± 0.01	No	E152I	−	−1.78 ± 0.25	No
N94K	−	−0.11 ± 0.01	No	E152W	−	−1.04 ± 0.14	No
N94M	−	−0.11 ± 0.01	No	E152L	−	−0.95 ± 0.10	No
N94P	−	NF	No	E152M	−	−0.83 ± 0.07	No
N94R	−	NF	No	Wt	−	−0.74 ± 0.05	No
N94T	−	NF	No	E152Y	−	−0.62 ± 0.09	No
N94V	−	NF	No	E152F	−	−0.60 ± 0.08	No
N94Q	−	NF	No	E152C	−	−0.27 ± 0.02	No
N94I	−	NF	No	E152P	−	−0.09 ± 0.01	No
N94C	−	NF	No	E152N	−	NF	No
N94A	−	NF	No	E152K	−	NF	No
N94G	−	NF	No	E152R	−	NF	No
S177D	−	−15.69 ± 1.61	Yes	V188**G**	+	−21.84 ± 0.66	No
S177**I**	+	−14.03 ± 1.69	No	V188**Q**	+	−21.74 ± 0.49	No
S177G	−	−13.09 ± 0.35	Yes	V188**N**	+	−21.51 ± 0.51	No
S177F	−	−12.75 ± 1.51	Yes	V188**S**	+	−21.00 ± 0.91	No
S177W	−	−11.30 ± 0.11	Yes	V188**P**	+	−19.68 ± 0.80	No
S177**L**	+	−10.81 ± 1.73	No	V188**C**	+	−19.59 ± 0.73	No
S177P	−	−10.67 ± 0.99	Yes	V188**E**	+	−19.59 ± 0.77	No
S177Y	−	−10.60 ± 1.30	Yes	V188**H**	+	−18.50 ± 0.90	No
S177**V**	+	−10.20 ± 1.92	No	V188**T**	+	−15.83 ± 0.80	No
S177N	−	−9.61 ± 0.99	Yes	V188**D**	+	−11.87 ± 0.67	No
S177**T**	+	−8.96 ± 0.47	No	V188**K**	+	−10.43 ± 1.14	No
S177**C**	+	−8.19 ± 1.46	No	V188**A**	+	−10.37 ± 1.18	No
S177H	−	−8.17 ± 0.16	Yes	V188**R**	+	−10.02 ± 0.40	No
S177R	−	−6.97 ± 0.37	No	V188W	+/−	−8.41 ± 0.42	No
S177M	−	−4.71 ± 0.44	No	V188M	+/−	−5.84 ± 0.54	No
S177K	−	−2.62 ± 0.40	No	V188L	−	−3.11 ± 0.72	No
S177E	−	−2.14 ± 0.25	No	Wt	−	−1.40 ± 0.20	No
Wt	−	−0.55 ± 0.03	No	V188Y	+/−	−1.01 ± 0.10	No
S177Q	−	−0.37 ± 0.7	No	V188F	−	−0.20 ± 0.04	No
S177A	−	−0.17 ± 0.01	No	V188I	−	−0.10 ± 0.01	No

Patterns of amino acid substitutions of N94, E152, S177, and V188. Twenty mutations at each position were injected and measured as a set in a single batch of oocytes; thus, the range of wild-type currents in the four sets reflects the variation of expression in different batches of oocytes. Currents were recorded in 90Na and 90K bath solution. Mutants expressing currents that were indistinguishable from leak (<30 nA) are indicated as nonfunctional (NF). Amino acid substitutions that both rescued the yeast K^+ uptake–deficient phenotype and expressed large currents in *Xenopus* oocytes are shown in bold type.

In general, the structural environment of a transmembrane segment of a pore-lining subunit can be categorized as lipid facing, pore facing, or protein-interior facing (Choe et al., 1995; Collins et al., 1997; Minor et al., 1999). Our observations indicate that V188 in the open state occupies a pore-lining position so that all 20 amino acids can occupy the V188 position in the open channel. The limited tolerance for substitution of V188 in channels that remain closed in the absence of active G protein subunits, on the other hand, suggests that this position faces the interior of the channel protein in the closed state, so that only hydrophobic residues of a particular size range can be accommodated.

We also examined the tolerance of the other three residues identified in our yeast mutant screen for amino acid substitutions (Table 2). In contrast to V188, N94 was highly intolerant of substitutions. Only H and F were compatible with constitutively active channels that support yeast growth. Other substitution mutants failed to rescue yeast and displayed no detectable currents in *Xenopus* oocytes. In general, there was a good correlation between complementation in the yeast assay and large current expression in *Xenopus* oocytes. This is remarkable given the vast differences in the two assays.

At E152, D and Q gave rise to large K^+ currents, while changes to I, L, V, T, and C at S177 led to active K^+ channels. These mutants also rescued yeast growth. Interestingly, many other mutations of E152 and S177 expressed large currents in oocytes but did not rescue in yeast. These mutant channels displayed inward currents in 90Na/0K bath, indicating that K^+ selectivity was disrupted. By contrast, mutations at N94 or V188 did not significantly alter K^+ selectivity (Table 2), though substitutions of V188 with basic residues altered current kinetics (Figure 3B). For some mutations of E152 and S177, currents in 90Na were comparable to those ob-

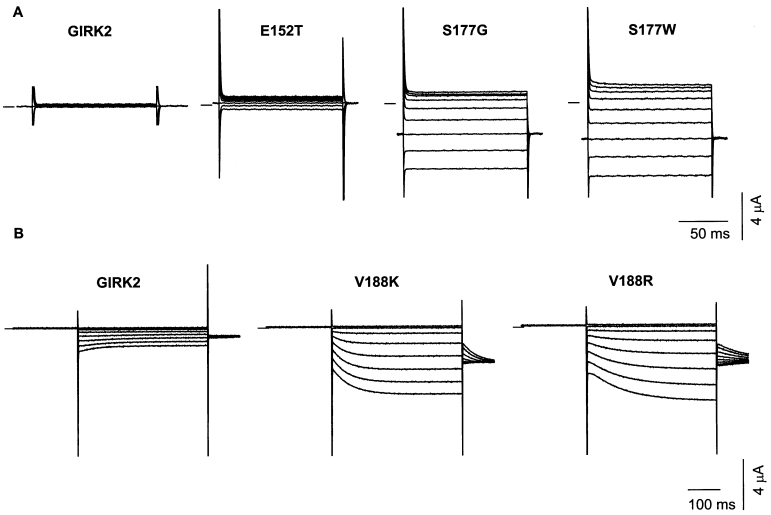

Figure 3. Mutations Affect Ion Selectivity and Time-Dependent Activation of GIRK2

(A) Representative current traces of GIRK2, GIRK2 E152T, GIRK2 S177G, and GIRK2 S177W were elicited with voltage pulses from +60 mV to −100 mV (20 mV increments) in 90Na/0K bath solution. Dash indicates the zero current level. The inward current in 90Na/0K bath solution indicates that these mutants allow Na^+ ions to enter the cell, distinct from wild-type GIRK2.

(B) Following jumps to negative potentials, mutations at V188 to K or R produced channels that display a slower time course of current activation relative to wild-type GIRK2, which exhibits a time-dependent decay. After jumping to −100 mV from a holding potential of 0 mV, this component could be fitted by a single exponential function with a time constant of 33.2 ms in V188K and 68.0 ms in V188R. Current traces were obtained by holding the membrane potential at 0 mV for 500 ms (truncated) and then pulsing from +10 mV to −130 mV (in 20 mV increments) for 400 ms.

served in 90K bath (e.g., S177G, $I_{Na}/I_K = 0.44 \pm 0.01$ [n = 6]; S177W, $I_{Na}/I_K = 0.50 \pm 0.02$ [n = 5]; Figure 3A). The large currents in oocytes may conceivably arise from activation of the mutant GIRK2 channels by intracellular Na^+ (Ho and Murrell-Lagnado, 1999; Petit-Jacques et al., 1999). One possible reason these mutants did not complement yeast may be that this yeast strain does not tolerate channels permeable to cations other than K^+. *Xenopus* oocytes can also be affected by the expression of nonselective ion channels. As reported with the GIRK2 *weaver* mutant (Navarro et al., 1996), oocytes injected with E152 or S177 mutants with altered potassium selectivity displayed a decreased survival compared to uninjected controls or GIRK2 mutants with intact potassium selectivity. Thus, mutations of the outer pair, E152 and S177, are similar in two ways. First, the gating mutations recovered from the yeast screen show similar single-channel properties, in kinetics as well as the appearance of subconductance states. Second, more drastic mutations at either position abolish potassium selectivity. The possible significance of these similarities will be discussed later.

Effects of Double Mutations

We considered whether the inner pair, N94 and V188, might interact or affect the same gating process by examining the phenotypes of double mutants. If two mutations affect different processes, then, in combination, one would expect to see evidence of additive effects. Alternatively, if two mutations affected the same process, then a mutation at one position may suppress or occlude the effects of the other. As a test of this principle, we constructed the double mutant containing E152D from the outer pair and V188G from the inner pair. The NP_o and the frequency of opening of the E152D V188G double mutant were much greater than those of the single mutants; they were roughly the sum of the latter ($NP_o = 10.01\% \pm 5.52\%$, $p < 0.05$; $f = 70.54 \pm 37.32\ s^{-1}$, $p < 0.05$) as one would predict for two mutations that act independently on separate processes (Figure 4A).

Possible interaction between the inner pair of N94 and V188 was examined by constructing the double mutant of two gating mutants, N94H and V188G, as well as the double mutant of N94H and V188I. The V188I mutant channels displayed basal currents smaller than wild type GIRK2 (Table 2) but could still be activated by coexpressed $G\beta\gamma$ (data not shown). Single-channel recordings of the N94H V188I double mutant revealed that V188I markedly suppressed the appearance of the long burst-like openings that were observed with N94H (Figure 4A). This suppression is manifested by decreases in the frequency of opening ($f = 1.42 \pm 0.28\ s^{-1}$) and mean open time ($0.69 \pm 0.46$ ms, $p = 0.0002$) causing a 30-fold reduction in open probability ($NP_o = 0.15\% \pm 0.09\ \%$, $p < 0.05$). Therefore, V188I is a second-site suppressor of the gating mutation N94H. This suppression was also apparent in the yeast complementation assay (Figure 4B). In contrast to the additive effects of the gating mutations E152D and V188G, no additive effects were observed in the N94H V188G double mutant, suggesting that V188G and N94H may affect the same gating process (Figure 4A).

Discussion

In this paper, we report the use of a yeast genetic screen as a nonbiased method of screening hundreds of thousands of clones for mutations that affect the gating of GIRK2. Remarkably, although mutations were generated randomly throughout the entire GIRK2 sequence, we have isolated the first gating mutations within M1, the P loop, and M2 of the transmembrane domain. This suggests that the conformational changes associated with GIRK2 channel gating occur in the transmembrane domain. The binding site for $G\beta\gamma$ is thought to be located in cytoplasmic regions in the N and C terminus (Huang et al., 1997; Krapivinsky et al., 1998) along with other factors known to participate in GIRK channel activation (Petit-Jacques et al., 1999). The location of the gate within the transmembrane domain suggests a molecular model for $G\beta\gamma$ gating of GIRK2 similar to those proposed

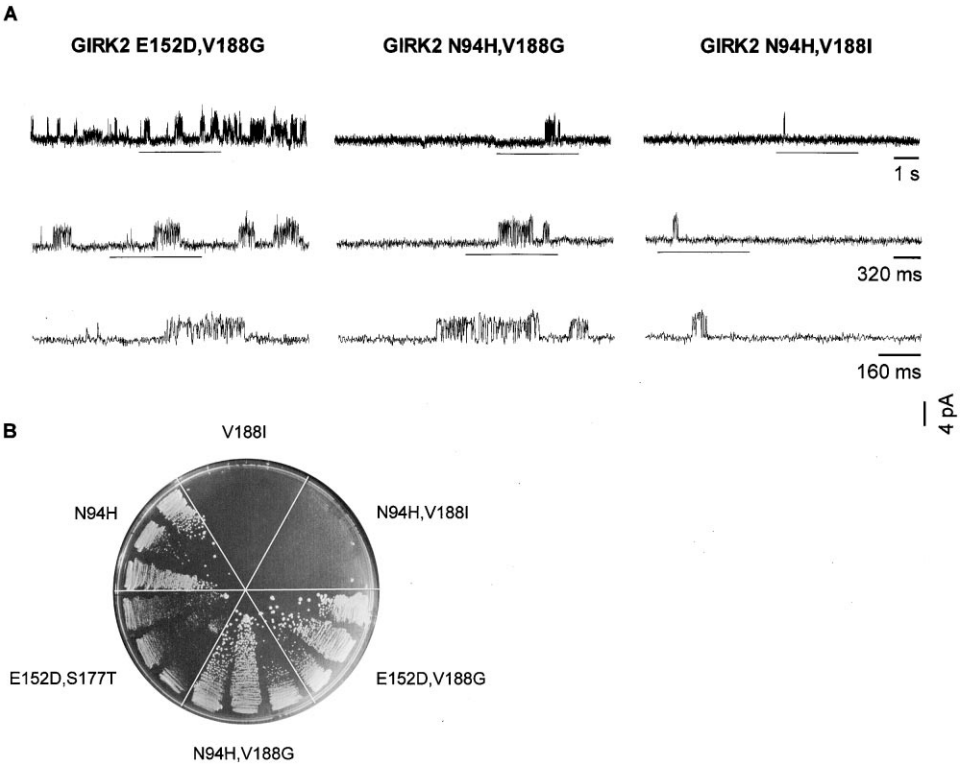

Figure 4. Different Double-Mutant GIRK2 Channels Display Additive or Suppressive Effects

(A) Representative single-channel recordings were taken in the cell-attached configuration from *Xenopus* oocytes at a holding potential of −100 mV. Channel openings are upward deflections. Bars indicate traces that are shown in expanded time scales.

(B) Yeast growth rescued by these double mutants correlate with their single-channel activities.

for the ATP inhibition of K_{ATP} channels (Drain et al., 1998; Tucker et al., 1998) and the activation of cyclic nucleotide-gated channels (Zong et al., 1998); i.e., the binding of second messengers to the cytoplasmic domains of the channel triggers gating motions in the transmembrane domain that lead to channel opening.

By developing a profile of amino acids that resulted in yeast rescue and high-current expression in *Xenopus* oocytes, we investigated the structural environment of each of the four positions in the open or closed state of GIRK2. At N94, E152, and S177, only a small number of amino acids led to functional, constitutively active K^+ channels. For V188, however, the majority of amino acid substitutions worked. The classification of positions in an ion channel as lipid facing, protein facing, or pore lining is based on energetics associated with stabilizing a protein structure in the lipid environment (Choe et al., 1995; Collins et al., 1997; Minor et al., 1999). For example, a position that tolerates substitutions to charged amino acids is likely to line the pore because of the unfavorable energetic costs of burying a charge within the lipid bilayer or within the protein itself, while lipid-facing positions are able to tolerate changes to any hydrophobic residues regardless of size or shape (Yeates et al., 1987; Minor et al., 1999). Residues involved in interactions between transmembrane segments, however, would be expected to display a limited tolerance for amino acids of a similar size and shape (Arkin et al., 1994). In general, past studies have used a limited set of changes or based their conclusions on the assumption that the transmembrane segments are fixed in a rigid structure. We have extended this approach to studies of channels that undergo considerable rotation and rearrangements during gating by using the yeast assay in conjunction with current measurements in *Xenopus* oocytes as a criterion to derive conclusions about the structure of the closed form or the open form. In this case, the profile of amino acids associated with active and inactive channels leads us to postulate that in the open state V188 faces the pore and can therefore tolerate substitution of all 19 amino acids, while in the closed state, this position faces the interior of the protein so that only hydrophobic residues of a particular size are tolerated. This suggests that, as GIRK channels open and close, M2 undergoes substantial rotation.

Even in the V188G gating mutant, which presumably has M2 in the open conformation due to the absence of a hydrophobic side chain that can fit into a hydrophobic pocket holding M2 in the close conformation, the open probability of the channel was <0.1. It thus seems likely that channel opening involves more than one gate. Besides V188 at the inner half of M2, the pore region including E152 appears to be involved in separate gating processes as indicated by the additive effects of E152D and V188G in the double-mutant studies (Figure 4). A review of prior studies of other inward rectifiers suggests a correspondence with the gating mutations identified here. N94 aligns with K80 in ROMK1 (Kir 1.1) that medi-

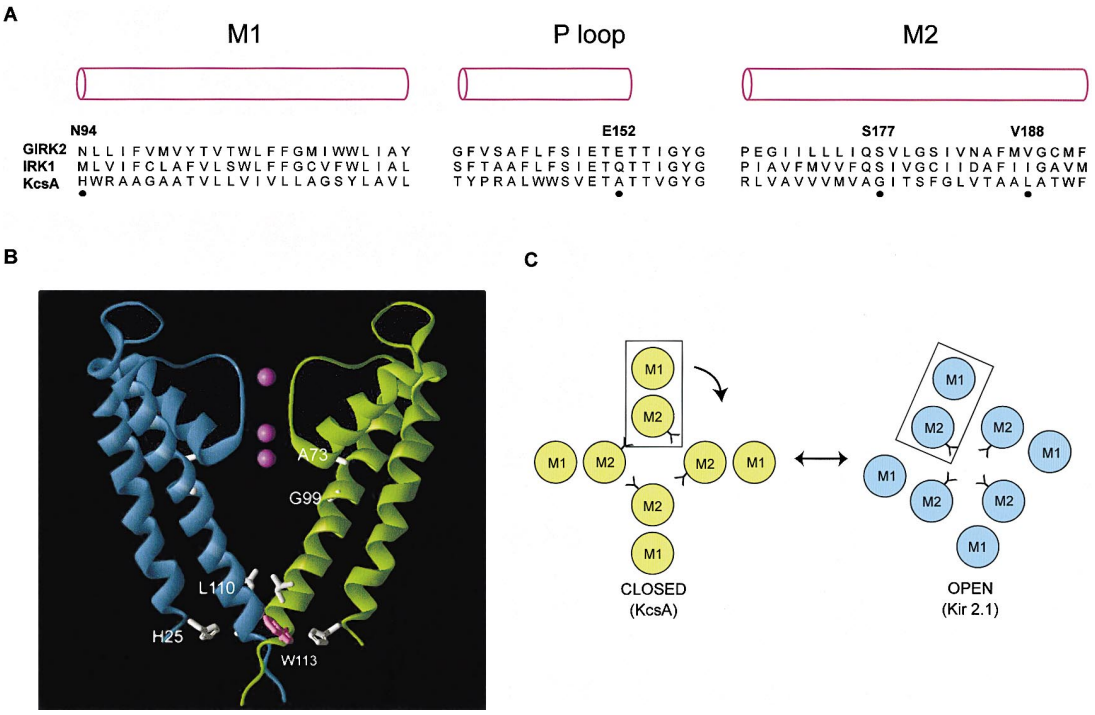

Figure 5. One Model of Gating Derived from an Open-State Model of IRK1 and the Known KcsA Structure

(A) Sequence alignment of M1 (aa 94–118), the P loop (aa 140–158), and M2 (aa 167–192) of GIRK2 with IRK1 and KcsA. There is weak sequence homology between the transmembrane regions of inward rectifiers and KcsA; the alignment of IRK1 (aa 84–108; 128–146; 155–180) and KcsA (aa 25–49; 61–79; 89–114) shown here is derived from a structural analysis of M1–M2 interactions (Minor et al., 1999), and the residues identified in the screen are indicated.

(B) A side view of the KcsA potassium channel (Doyle et al., 1998) showing two subunits depicted as blue and green ribbons. The corresponding amino acid positions identified in the yeast screen of GIRK2 mutants are drawn in white, and W113 is shown in red.

(C) A potential model of the transmembrane helical arrangement in the open form and the closed form. V188 (drawn) in the closed state aligns with a residue in KcsA that is involved in M2–M2 interactions; in IRK1, V188 is predicted to face the pore. During gating, M1 and M2 as a unit (boxed) may rotate clockwise bringing V188 from a buried position to a pore-lining position.

ates pH regulation of these channels (Fakler et al., 1996). E152 in the P loop is equivalent to position Q140 in IRK1 that affects fast gating (Guo and Kubo, 1998), and S177 of GIRK2 (corresponding to S166 in GIRK1) is equivalent to S165 in IRK1, a position recently reported to be involved in intracellular block by Rb^+ and Cs^+ (Thompson et al., 2000) (Figure 5A). V188 is equivalent to I176 in IRK1, a pore-facing position in the transmembrane structure derived from yeast mutational analysis (Minor et al., 1999) and reactivity to modifying agents (Lu et al., 1999). This is consistent with the substitution pattern seen with V188 and the notion that the transmembrane structure of IRK1 represents the open form. Why is it that isoleucine at position 188 allows GIRK2 channels to remain closed whereas IRK1 with isoleucine at the equivalent position stays open? One possible explanation is that the equivalent positions of N94 (M84 in IRK1) and E152 (Q140 in IRK1) are occupied by residues that are only compatible with constitutively active channels. Indeed, the E152Q mutant GIRK2 channels exhibit large basal currents (Table 2), and it may be of interest to determine whether the N94M V188I double mutant of GIRK2 is constitutively active. It is also possible that other differences between IRK1 and the V188I mutant GIRK2 channel contribute to their different gating properties. In KcsA, V188 aligns with L110, which does not line the pore but is buried in protein–protein interactions between adjacent M2s (Minor et al., 1999). Interestingly, L110 and H25 (corresponding to N94 in GIRK2) make contacts with the same residue, W113, in the same KcsA subunit (Figure 5B). This provides a plausible explanation for the strong interaction between N94 and V188 that was observed in GIRK2 (Figure 4).

Given that S165 in IRK1 as well as the corresponding S177 residue in GIRK2 are tolerant of substitutions in their open state and likely line the pore, how might S177 contribute to gating of the GIRK2 channel? One possible explanation is that S177 in the closed GIRK2 channel does not face the pore but rather interacts with other residues within the channel protein. One potential model for the closed GIRK2 channel is the structure of KcsA at pH 7, since the KcsA channel is open at low pH but closed at pH 7 (Heginbotham et al., 1999; Perozo et al., 1999). In this study, GIRK2 E152 and S177 were linked by their susceptibility to mutations that cause constitutive activation (Figure 1A; Table 1) and/or a loss of K^+ selectivity (Table 2; Figure 3A) and the similar kinetic properties and the occurrence of subconductance states in their respective gating mutants (Figure 2A). GIRK2 E152 aligns with KcsA A73, which is in the pore helix, while GIRK2 S177 aligns with KcsA G99, which is in M2 and positioned to interact with A73 (Figure 5B). Thus, the KcsA model provides plausible explanations for the similar mutant phenotypes of the outer pair, E152 and S177,

as well as the strong interaction between the inner pair, N94 and V188, in the double-mutant studies. The structure also illustrates how mutations at S177, outside the canonical selectivity filter, can disrupt K^+ selectivity and how conformational changes in the P loop may influence gating.

The conformational change that allows a closed GIRK channel to open would then be expected to involve a clockwise rotation of the M2 helix, when viewed from outside the cell (Figure 5C). V188 moves from a buried position corresponding to L110 in KcsA (Doyle et al., 1998) to a pore-lining position corresponding to I176 in Kir2.1 (Minor et al., 1999). We speculate that the entire subunit moves as a unit during which contacts between M1 and M2 of the same subunit are preserved (Doyle et al., 1998; Minor et al., 1999). This model necessarily raises questions about how this motion might affect the positioning of the pore helices and the backbone carbonyls in the P loop that are thought to form binding sites for K^+ ions (Doyle et al., 1998; Roux and MacKinnon, 1999; Aqvist and Luzhkov, 2000). One possibility is that the movement of M1 and M2 is made relative to the pore network and pore helix, so that S177 would interact with the pore helix in the closed channel but face the pore in the open channel. Given that external K^+ ions play important roles in controlling the conformation of the P region (Baukrowitz and Yellen, 1995; Loots and Isacoff, 1998), it seems plausible that the pore loop and pore helix may not move in unison with the transmembrane helices. It is conceivable, however, that the P loop undergoes more subtle movements. In fact, fast gating is affected by unnatural amino acid substitutions that reduce the polarity of the backbone carbonyls of the GYG motif in the P loop (Lu et al., 2001). Furthermore, permeant ions in the pore are known to affect K^+ channel gating (Swenson and Armstrong, 1981; Neyton and Pelleschi, 1991; Demo and Yellen, 1992). It remains possible that channel gating involves movements of not only the last transmembrane segment but also the selectivity filter formed by the P loop as supported by studies of the voltage-gated K^+ channels (Chapman et al., 1997; Zheng and Sigworth, 1997; Zheng and Sigworth, 1998).

Here, we report the identification of mutations in a yeast genetic screen that confers constitutive activity onto a G protein–activated potassium channel without altering ion selectivity or rectification properties. Random mutagenesis combined with a functional screen in yeast makes possible an unbiased analysis of hundreds of thousands of mutant clones for mutations anywhere within GIRK2 that promote channel opening. The emergence from this yeast screen of gating mutations in the transmembrane domain implicates the transmembrane helices as well as the P loop as the primary machineries that open and close the GIRK channel. The value of a large-scale genetic screen for gating mutations is underscored by the identification of novel mutations—outside of the regions previously identified as involved in gating—that can be the subject of further studies.

Experimental Procedures

Molecular Biology and DNA Shuffling

DNA shuffling of GIRK2, a gift from M. Lazdunski (Lesage et al., 1994), was performed essentially as described (Stemmer, 1994) and cloned into a derivative of pYES2 harboring the Met-25 promoter (Minor et al., 1999). A sample of the library of ~400,000 independent clones were sequenced and found to have an error rate of 0.5% with mutations in the same proportions as reported before. DNA backcrossing was performed using the same protocol as above except that reassembly was done using Pfu polymerase, which reduces the error rate to <0.01%. Capped cRNA was synthesized with Ampliscribe kit (Epicenter Technologies) after the constructs were moved into pGEMHE (Liman et al., 1992) containing an AflII restriction site for linearizing.

Yeast Complementation

Selection experiments were conducted in the yeast strain SGY1528 (MATa *ade*2-1 *can*1-100 *his*3-11,15 *leu*2-3,112 *trp*1-1 *ura*3-1 *trk*1::HIS3 *trk*2::TRP1), a gift of S. Kurtz. This strain was transformed with a library of randomly mutagenized GIRK2 and plated onto high-potassium plates made from standard -ura/-met dropout media with 100 mM KCl and titrated to pH 6.5 with Tris base. After 3 days of growth at 30°C, plates were replica plated onto plates containing 2 mM KCl. After 2 more days of growth, plates were replica plated again onto plates containing 0.1 mM KCl. Positive clones were verified by recovering the plasmid and transforming a second time. The low-potassium selective plates contained -ura/-met dropout powder, 1.5% SeaKem LE agarose (FMC), 1 mM $MgSO_4$, 50 μM $CaCl_2$, 1% dextrose, 0.81 mM H_3BO_3, 0.14 μM $Cu(II)SO_4 \cdot (H_2O)$, 0.6 μM KI, 1.8 μM $Fe(II)SO_4 \cdot (H_2O)_7$, 2.6 μM $MnSO_4$, 7.3 μM $(NH_4)_6Mo_7O_{24}$, 1.4 μM $ZnSO_4$, 8.1 nM biotin, 1.7 μM D-pantothenic acid hemicalcium salt, 3.2 μM nicotinic acid, 1.9 μM pyroxine•HCl, 1.2 μM thiamine, and 11 μM inositol and was titrated to pH 6.0 with H_3PO_4.

Electrophysiology

Two-electrode voltage-clamp currents (GeneClamp 500B, Axon Instruments, Foster City, CA) were measured 3–4 days after injection of stage V or VI oocytes with 25 ng of channel cRNA. All comparisons were made within the same batch of oocytes. Currents were routinely measured in 90K and 90Na bath solution. 90K bath solution contained 90 mM KCl, 1 mM $MgCl_2$, 10 mM HEPES, pH 7.5; 90Na bath solution contained 90 mM NaCl, 1 mM $MgCl_2$, 10 mM HEPES, pH 7.5. Single-channel currents were obtained using cell-attached patch-clamp recording (Hamill et al., 1981) at room temperature from oocytes 3–6 days after RNA injection. The vitelline membrane was removed before recordings. The recording electrodes were pulled from thin-walled borosilicate glass with an internal filament (MTW150F-3, World Precision Instruments) using a P-87 Flaming Brown puller (Sutter Instrument) and were fire polished to a resistance of 5–10 MΩ. The bath solution consisted of 110 mM KCl, 1.44 mM $MgCl_2$, 30 mM KOH, 10 mM EGTA, 10 mM HEPES, pH to 7.2. The intrapipette solution consisted of 140 mM KCl, 1.2 mM $MgCl_2$, 2.6 mM $CaCl_2$, 10 mM HEPES, pH to 7.4. The equilibrium potential for potassium ions was 0 mV. All patches were voltage-clamped at −100 mV intracellularly. Currents were recorded with Axopatch 200A patch-clamp amplifier (Axon Instruments) and were low-pass filtered (3 dB, 2 kHz) with an 8-pole Bessel filter (Frequency Devices). Single-channel data were acquired and digitized at 20 kHz online using Clampex 7 software (Axon) via a 16 bit A/D converter (Digidata acquisition board 1200A; Axon). Simultaneously, data were stored on VHS tapes using a JVC HR-J400U VCR and a PCM converter system (VR-10B; Instrutech). Digitized single-channel records were detected using Fetchan 6.05 (events list) of pCLAMP (Axon) taking a 50% threshold crossing criterion and analyzed with Interval5 (Dr. Barry S. Pallotta). Only patches with infrequent multiple-channel activity were used for analysis. Duration histograms were constructed as described by Sigworth and Sine (1987), and estimates of exponential areas and time constants were obtained using the method of maximal likelihood estimation. The number of exponential functions required to fit the duration distribution was determined by fitting increasing numbers of functions until additional components could not significantly improve the fit (Horn, 1987; McManus and Magleby, 1988). Mean durations were corrected for missed events by taking the sum of the relative area (a) of each exponential component in the duration frequency histogram obtained from the time constant (τ) of the corresponding component. All measurements are given as mean ± standard error of the mean.

Protein Preparation and Western Blotting

Total oocyte membranes were prepared essentially as described (Tucker et al., 1996). For each mutant, 12–15 oocytes were lysed by

pipetting up and down in ice-cold phosphate-buffered saline with protease inhibitors. The lysate was separated by centrifugation at 1000 g for 10 min at 4°C. The supernatant was transferred to a new tube, spun again, and collected. After adding one volume of SDS–PAGE sample buffer with 0.1 M DTT, the samples were heated to 50°C for 30 min and then frozen until SDS–PAGE. Blots were probed with a polyclonal antibody against an N-terminal region of GIRK2 (06-792; Upstate) at a concentration of 0.5 mg/ml and developed with ECL chemiluminescence using a donkey anti-rabbit horseradish peroxidase (HRP) as a secondary antibody.

Acknowledgments

We thank M. Lazdunski for the kind gift of GIRK2 cDNA; S. Kurtz for providing the yeast strain; B. Pecson and S. Albin for technical assistance; and D. Minor, B. Cohen, D. Ma, M. Margeta, K. Raab-Graham, M. Schonemann, B. Schwappach, and F. Yoshikawa for advice and comments. Y. N. J. and L. Y. J. are HHMI investigators. This work was supported by grants from the NIH (L. Y. J. and Y. N. J.).

Received October 31, 2000; revised January 22, 2001.

References

Arkin, I.T., Adams, P.D., MacKenzie, K.R., Lemmon, M.A., Brunger, A.T., and Engelman, D.M. (1994). Structural organization of the pentameric transmembrane α-helices of phospholamban, a cardiac ion channel. EMBO J. *13*, 4757–4764.

Aqvist, J., and Luzhkov, V. (2000). Ion permeation mechanism of the potassium channel. Nature *404*, 881–884.

Baukrowitz, T., and Yellen, G. (1995). Modulation of K^+ current by frequency and external [K^+]: a tale of two inactivation mechanisms. Neuron *15*, 951–960.

Capener, C.E., Shrivastava, I.H., Ranatunga, K.M., Forrest, L.R., Smith, G.R., and Sansom, M.S. (2000). Homology modeling and molecular dynamics simulation studies of an inward rectifier potassium channel. Biophys. J. *78*, 2929–2942.

Chapman, M.L., VanDongen, H.M.A., and VanDongen, A.M.J. (1997). Activation-dependent subconductance levels in the drk1 K^+ channel suggest a subunit basis for ion permeation and gating. Biophys. J. *72*, 708–719.

Choe, S., Stevens, C.F., and Sullivan, J.M. (1995). Three distinct structural environments of a transmembrane domain in the inwardly rectifying potassium channel ROMK1 defined by perturbation. Proc. Natl. Acad. Sci. USA *92*, 12046–12049.

Collins, A., Chuang, H., Jan, Y.N., and Jan, L.Y. (1997). Scanning mutagenesis of the putative transmembrane segments of Kir2.1, an inward rectifier potassium channel. Proc. Natl. Acad. Sci. USA *94*, 5456–5460.

Demo, S.D., and Yellen, G. (1992). Ion effects on gating of the Ca^{2+}-activated K^+ channels correlate with occupancy of the pore. Biophys. J. *61*, 639–648.

Doyle, D.A., Cabral, J.M., Pfuetzner, R.A., Kuo, A., Gulbis, J.M., Cohen, S.L., Chait, B.T., and MacKinnon, R. (1998). The structure of the potassium channel: molecular basis of K^+ conduction and selectivity. Science *280*, 69–77.

Drain, P., Li, L., and Wang, J. (1998). K_{ATP} channel inhibition by ATP requires distinct functional domains of the cytoplasmic C terminus of the pore-forming subunit. Proc. Natl. Acad. Sci. USA *95*, 13953–13958.

Fakler, B., Schultz, J.H., Yang, J., Schulte, U., Brandle, U., Zenner, H.P., Jan, L.Y., and Ruppersberg, J.P. (1996). Identification of a titratable lysine residue that determines sensitivity of kidney potassium channels (ROMK) to intracellular pH. EMBO J. *15*, 4093–4099.

Guatteo, E., Fusco, F.R., Giacomini, P., Bernardi, G., and Mercuri, N.B. (2000). The *weaver* mutation reverses the function of dopamine and GABA in mouse dopaminergic neurons. J. Neurosci. *20*, 6013–6020.

Guo, L., and Kubo, Y. (1998). Comparison of the open-close kinetics of the cloned inward rectifier K^+ channel IRK1 and its point mutant (Q140E) in the pore region. Receptors Channels *5*, 273–289.

Hamill, O.P., Marty, A., Neher, E., Sakmann, B., and Sigworth, F.J. (1981). Improved patch-clamp techniques for high-resolution current recording from cells and cell-free membrane patches. Pflugers Arch. *391*, 85–100.

He, C., Zhang, H., Mirshahi, T., and Logothetis, D.E. (1999). Identification of a potassium channel site that interacts with G proteinβγ subunits to mediate agonist-induced signaling. J. Biol. Chem. *274*, 12517–12524.

Heginbotham, L., LeMasurier, M., Kolmakova-Partensky, L., and Miller, C. (1999). Single *Streptomyces lividans* K^+ channels: functional asymmetries and sidedness of proton activation. J. Gen. Physiol. *114*, 551–560.

Ho, I.M., and Murrell-Lagnado, R.D. (1999). Molecular determinants for sodium-dependent activation of G protein-gated K^+ channels. J. Biol. Chem. *274*, 8639–8648.

Horn, R. (1987). Statistical methods for model discrimination. Applications to gating kinetics and permeation of the acetylcholine receptor channel. Biophys. J. *51*, 255–263.

Huang, C.L., Jan, Y.N., and Jan, L.Y. (1997). Binding of the G protein βγ subunit to multiple regions of G protein-gated inward-rectifying K^+ channels. FEBS Lett. *405*, 291–298.

Huang, C.L., Feng, S., and Hilgemann, D.W. (1998). Direct activation of inward rectifier potassium channels by PIP_2 and its stabilization by Gβγ. Nature *391*, 803–806.

Ivanova-Nikolova, T.T., and Breitwieser, G.E. (1997). Effector contributions to Gβγ-mediated signaling as revealed by muscarinic potassium channel gating. J. Gen. Physiol. *109*, 245–253.

Ivanova-Nikolova, T.T., Nikolov, E.N., Hansen, C., and Robishaw, J.D. (1998). Muscarinic K^+ channel in the heart. Modal regulation by G protein βγ subunits. J. Gen. Physiol. *112*, 199–210.

Jan, L.Y., and Jan, Y.N. (1997). Cloned potassium channels from eukaryotes and prokaryotes. Annu. Rev. Neurosci. *20*, 91–123.

Kennedy, M.E., Nemec, J., Corey, S., Wickman, K., and Clapham, D.E. (1999). GIRK4 confers appropriate processing and cell surface localization to G-protein-gated potassium channels. J. Biol. Chem. *274*, 2571–2582.

Ko, C.H., and Gaber, R.F. (1991). TRK1 and TRK2 encode structurally related K^+ transporters in *Saccharomyces cerevisiae*. Mol. Cell. Biol. *11*, 4266–4273.

Krapivinsky, G., Kennedy, M.E., Nemec, J., Medina, I., Krapivinsky, L., and Clapham, D.E. (1998). Gβγ binding to GIRK4 subunit is critical for G protein-gated K^+ channel activation. J. Biol. Chem. *273*, 16946–16952.

Kubo, Y., Baldwin, T.J., Jan, Y.N., and Jan, L.Y. (1993). Primary structure and functional expression of a mouse inward rectifier potassium channel. Nature *362*, 127–133.

Lesage, F., Duprat, F., Fink, M., Guillemare, E., Coppola, T., Lazdunski, M., and Hugnot, J.P. (1994). Cloning provides evidence for a family of inward rectifier and G-protein coupled K^+ channels in the brain. FEBS Lett. *353*, 37–42.

Liman, E.R., Tytgat, J., and Hess, P. (1992). Subunit stoichiometry of a mammalian K^+ channel determined by construction of multimeric cDNAs. Neuron *9*, 861–871.

Liu, Y., Holmgren, M., Jurman, M.E., and Yellen, G. (1997). Gated access to the pore of a voltage-dependent K^+ channel. Neuron *19*, 175–184.

Loots, E., and Isacoff, E.Y. (1998). Protein rearrangements underlying slow inactivation of the Shaker K^+ channel. J. Gen. Physiol. *112*, 377–389.

Lu, T., Nguyen, B., Zhang, X., and Yang, J. (1999). Architecture of a K^+ channel inner pore revealed by stoichiometric covalent modification. Neuron *22*, 571–580.

Lu, T., Ting, A.Y., Mainland, J., Jan, L.Y., Schultz, P.G., and Yang, J. (2001). Probing ion permeation and gating in a K^+ channel with backbone mutations in the selectivity filter. Nat. Neurosci., in press.

Luchian, T., Dascal, N., Dessauer, C., Platzer, D., Davidson, N., Lester, H.A., and Schreibmayer, W. (1997). A C-terminal peptide of the GIRK1 subunit directly blocks the G protein-activated K^+ channel (GIRK) expressed in *Xenopus* oocytes. J. Physiol. *505*, 13–22.

Lüscher, C., Jan, L.Y., Stoffel, M., Malenka, R.C., and Nicoll, R.A. (1997). G protein-coupled inwardly rectifying K^+ channels (GIRKs) mediate postsynaptic but not presynaptic transmitter actions in hippocampal neurons. Neuron *19*, 687–695.

MacKinnon, R., Cohen, S.L., Kuo, A., Lee, A., and Chait, B.T. (1998). Structural conservation in prokaryotic and eukaryotic potassium channels. Science *280*, 106–109.

McManus, O.B., and Magleby, K.L. (1988). Kinetic states and modes of single large-conductance calcium-activated potassium channels in cultured rat skeletal muscle. J. Physiol. *402*, 79–120.

Minor, D.L., Jr., Masseling, S.J., Jan, Y.N., and Jan, L.Y. (1999). Transmembrane structure of an inwardly rectifying potassium channel. Cell *96*, 879–891.

Navarro, B., Kennedy, M.E., Velimirovíc, B., Bhat, D., Peterson, A.S., and Clapham, D.E. (1996). Nonselective and G $\beta\gamma$-insensitive weaver K^+ channels. Science *272*, 1950–1953.

Nemec, J., Wickman, K., and Clapham, D.E. (1999). G$\beta\gamma$ binding increases the open time of I_{KACh}: kinetic evidence for multiple G$\beta\gamma$ binding sites. Biophys. J. *76*, 246–252.

Neyton, J., and Pelleschi, M. (1991). Multi-ion occupancy alters gating in high-conductance, Ca^{2+}-activated K^+ channels. J. Gen. Physiol. *97*, 641–655.

Perozo, E., Cortes, D.M., and Cuello, L.G. (1999). Structural rearrangements underlying K^+-channel activation gating. Science *285*, 73–78.

Petit-Jacques, J., Sui, J.L., and Logothetis, D.E. (1999). Synergistic activation of G protein-gated inwardly rectifying potassium channels by the $\beta\gamma$ subunits of G proteins and Na^+ and Mg^{2+} ions. J. Gen. Physiol. *114*, 673–684.

Pessia, M., Bond, C.T., Kavanaugh, M.P., and Adelman, J.P. (1995). Contributions of the C-terminal domain to gating properties of inward rectifier potassium channels. Neuron *14*, 1039–1045.

Roux, B., and MacKinnon, R. (1999). The cavity and pore helices in the KcsA K^+ channel: electrostatic stabilization of monovalent cations. Science *285*, 100–102.

Sigworth, F.J., and Sine, S.M. (1987). Data transformations for improved display and fitting of single-channel dwell time histograms. Biophys. J. *52*, 1047–1054.

Stemmer, W.P. (1994). DNA shuffling by random fragmentation and reassembly: in vitro recombination for molecular evolution. Proc. Natl. Acad. Sci. USA *91*, 10747–10751.

Sui, J.L., Petit-Jacques, J., and Logothetis, D.E. (1998). Activation of the atrial I_{KACh} channel by the $\beta\gamma$ subunits of G proteins or intracellular Na^+ ions depends on the presence of phosphatidylinositol phosphates. Proc. Natl. Acad. Sci. USA *95*, 1307–1312.

Swenson, R.P., and Armstrong, C.M. (1981). K^+ channels close more slowly in the presence of external K^+ and Rb^+. Nature *291*, 427–429.

Tang, W., Ruknudin, A., Yang, W.P., Shaw, S.Y., Knickerbocker, A., and Kurtz, S. (1995). Functional expression of a vertebrate inwardly rectifying K^+ channel in yeast. Mol. Biol. Cell *6*, 1231–1240.

Thompson, G.A., Leyland, M.L., Ashmole, I., Sutcliffe, M.J., and Stanfield, P.R. (2000). Residues beyond the selectivity filter of the K^+ channel Kir2.1 regulate permeation and block by external Rb^+ and Cs^+. J. Physiol. *526 (pt. 2)*, 231–240.

Tucker, S.J., Bond, C.T., Herson, P., Pessia, M., and Adelman, J.P. (1996). Inhibitory interactions between two inward rectifier K^+ channel subunits mediated by the transmembrane domains. J. Biol. Chem. *271*, 5866–5870.

Tucker, S.J., Gribble, F.M., Proks, P., Trapp, S., Ryder, T.J., Haug, T., Reimann, F., and Ashcroft, F.M. (1998). Molecular determinants of K_{ATP} channel inhibition by ATP. EMBO J. *17*, 3290–3296.

Wickman, K.D., Iñiguez-Lluhl, J.A., Davenport, P.A., Taussig, R., Krapivinsky, G.B., Linder, M.E., Gilman, A.G., and Clapham, D.E. (1994). Recombinant G-protein $\beta\gamma$-subunits activate the muscarinic-gated atrial potassium channel. Nature *368*, 255–257.

Wickman, K., Nemec, J., Gendler, S.J., and Clapham, D.E. (1998). Abnormal heart rate regulation in GIRK4 knockout mice. Neuron *20*, 103–114.

Yakubovich, D., Pastushenko, V., Bitler, A., Dessauer, C.W., and Dascal, N. (2000). Slow modal gating of single G protein-activated K^+ channels expressed in *Xenopus* oocytes. J. Physiol. *524 (pt. 3)*, 737–755.

Yeates, T.O., Komiya, H., Rees, D.C., Allen, J.P., and Feher, G. (1987). Structure of the reaction center from *Rhodobacter sphaeroides* R-26: membrane-protein interactions. Proc. Natl. Acad. Sci. USA *84*, 6438–6442.

Zheng, J., and Sigworth, F.J. (1997). Selectivity changes during activation of mutant *shaker* potassium channels. J. Gen. Physiol. *110*, 101–117.

Zheng, J., and Sigworth, F.J. (1998). Intermediate conductances during deactivation of heteromultimeric *shaker* potassium channels. J. Gen. Physiol. *112*, 457–474.

Zong, X., Zucker, H., Hofmann, F., and Biel, M. (1998). Three amino acids in the C-linker are major determinants of gating in cyclic nucleotide-gated channels. EMBO J. *17*, 353–362.